Variable-Speed Prime Mover Driving Three-Phase Self-Excited Induction Generator with Static VAR Compensator Voltage Regulation –Part I : Theoretical Performance Analysis–

Tarek Ahmed*, Schinichro Nagai*, Koji Soshin*, Eiji Hiraki* and Mutsuo Nakaoka*

Abstract - This paper deals with the nodal admittance approach steady-state frequency domain analysis of the three-phase self-excited induction generator (SEIG) driven by the variable speed prime mover as the wind turbine. The steady-state performance analysis of this power conditioner designed for the renewable energy is based on the principle of equating the input mechanical power of the three-phase SEIG to the output mechanical power of the variable speed prime mover mentioned above. Using the approximate frequency domain based equivalent circuit of the three-phase SEIG. The main features of the present algorithm of the steady-state performance analysis of the three-phase SEIG treated here are that the variable speed prime mover characteristics are included in the approximate equivalent circuit of the three-phase SEIG under the condition of the speed changes of the prime mover without complex computations processes.
Furthermore, a feedback closed-loop voltage regulation of the three-phase SEIG as a power conditioner which is driven by variable speed prime movers such as the wind turbine(WT) employing the static VAR compensator(SVC) circuit composed of the thyristor phase controlled reactor(TCR) and the thyristor switched capacitor(TSC) controlled by the PI controller is designed and considered for wind-turbine driving power conditioner.

Keywords: three-phase self-excited induction generator, static VAR compensator, thyristor phase controlled reactor, thyristor switched capacitor, feedback terminal voltage regulation scheme, power conditioner, variable-speed prime mover, rural renewable energy and wind turbine-based dc motor modeling

1. Introduction

From an earth environment point of view, solar photovoltaic power generation, wind turbine power generation and wave turbine power generation have attracted special interests for renewable and sustainable energy in the rural region. Of these, the AC generator driven by the wind turbine which is typically divided into two; synchronous and induction types has been widely used for utility AC power interactive and stand-alone systems. The three-phase induction machine with squirrel cage rotor or wound rotor could work as a three-phase induction generator either it is connected to a utility AC power distribution line supply or operate in the self-excitation mode due to the terminal excitation capacitors. The generated terminal voltage and the frequency of the three-phase induction generator are the same as the grid voltage and the commercial frequency of the utility AC power source to which the three-phase induction generator with the utility interactive transformer or reactor is connected. The reactive power required for the three-phase induction generator is to be supplied by the utility AC power source and the active output power of the three-phase induction generator is delivered to the utility AC power source. With a fixed frequency dictated by the utility AC power source, the three-phase induction machine starts to become a generation mode when the rotor shaft speed is above the synchronous speed. The operating range of the rotor shaft speed is also limited by the slip of the induction machine. In case of a very high slip, the winding copper losses increase as the current increases. On the other hand, in an isolated stand-alone operation in the rural energy utilization area, the three-phase induction generator can operate in self-excitation capacitor mode due to the fixed terminal capacitor. The three-phase self-excited induction generator(SEIG) determines its own generated terminal voltage and frequency which strongly depend on the capacitance of the excitation capacitor, the three-phase induction machine circuit parameters, the electrical load constants, and the variable speed of the prime mover. The

* Dept. of Electrical and Electronic Engineering, Yamaguchi University, Japan. (tarek@pe-news1.eee.yamaguchi-u.ac.jp)
Received January 4, 2003 ; Accepted Febryary 10, 2003

operating speed of the three-phase SEIG generator is extended without generating excessive loss. The induction generator with squirrel cage rotor has some advantageous merits, low cost, simple structure, ruggedness and low inertia and easy to connect to the utility. The renewable and sustainable energy resources in the rural region such as the wind energy, the water falling and the wave attitude energy are made use of driving the three-phase SEIG to build up the generated terminal voltage via connecting the excitation capacitor bank. The approximate steady-state analysis in a frequency domain of the three-phase SEIG has been done with the following assumptions for some papers presented previously[1-12],

- Iron losses are negligible
- Only Fundamental M.M.F. waves are considered
- Resistance and inductances of the induction machine are constant, except for the magnetizing inductance. This one can be described graphically by means of the no-load curve.
- The rate of change in the parameters and variables of the equivalent circuit is very small, so that the steady-state equivalent circuit can be used. Because of the operation on an isolated network with variable rotor shaft speed, the frequency of the output voltage can no longer be kept constant. These variations affect to both the reactances and the value of slip for a given speed. To take account of these variations, all reactances are represented in per unit terms referred to the values measured at the base frequency (50 Hz), so that any reactance at a given frequency can be denoted by $X=X_{base}*f$, where X is the reactance in ohm at the output frequency F of the three-phase SEIG, X_{base} is the reactance at 50 Hz and f=F/50 is the per unit frequency

By dividing all circuit parameters and voltages denoted by f, the following equivalent circuit is obtained. In this circuit the slip is defined in terms of the relative frequency f and the relative rotor speed ν where (ν=N/Ns), N is the rotor speed in rpm and Ns is the synchronous speed =1500.0 rpm for 50Hz.

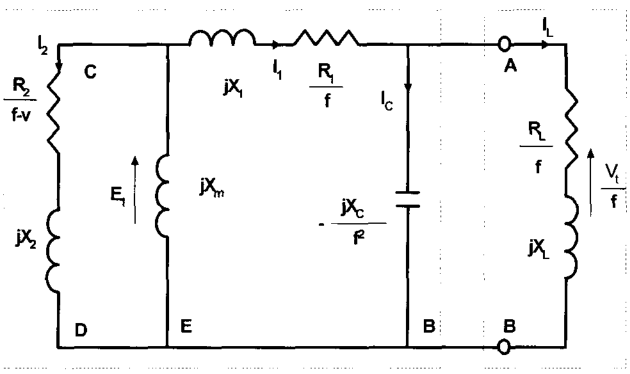

Fig. 1 Per-phase equivalent circuit of the three-phase self-excited induction generator

From Fig.1, R_1, X_1, R_2 and X_2 are the resistances and the leakage reactances of the stator winding and the rotor winding referred to the stator winding side in ohm, respectively, R_L and X_L are the resistance and the reactance of the load in ohm, respectively, C is the excitation capacitor capacitance in farad, X_c is the excitation capacitive reactance in ohm, X_m is the magnetizing reactance in ohm, and E_1, V_t, I_1, I_2, I_L and I_C are the per-phase air gap voltage, the per-phase terminal output voltage, the per-phase stator current, the per-phase rotor current referred to the stator side, the per-phase load current and the per-phase excitation current of the three-phase SEIG, respectively.

This paper presents an analytical study by utilizing a nodal admittance approach to illustrate the operation of the three SEIG driven by a variable speed prime mover in isolated stand-alone operation. The steady-state performance calculations are presented to support the frequency domain analysis. In addition, a closed loop PI compensator for the terminal voltage regulation of the three-phase SEIG driven directly by a variable speed prime mover is established using the SVC composed of thyristor phase controlled reactor; TCR and thyristor switched capacitor; TSC.

Possible and effective applications for the power conditioning system in variable-speed generation are currently under investigation. The generated output terminal voltage can be directly connected to load facilities and equipments are non-sensitive to the frequency, which includes a heater, a battery charger, a double converter etc. as well as can be connected to a converter to get a fixed-frequency AC output.

2. Voltage Regulation System Description for Three-Phase SEIG with PI controller-based SVC

With great advances of the power electronic semiconductor switching devices such as the planar gate IGBT, the trench gate controlled IGBTs as CSTBT and IEGT and static induction power devices; SIT, SITHs, and IGCT a reactive power controlling device called static VAR compensator is used effectively. That power controlling device replaces the conventional mechanical synchronous ac motors or VAR compensator operates with mechanical contact switches as well as instantaneous reactive compensator with current controlled voltage source inverter. The schematic line diagram of the three-phase SEIG voltage regulation used the SVC composed of the TCR and the TSC which is controlled by a PI compensator is shown in Fig.2, the three-phase 4 poles, 220 V, 2 kW, Y connected induction generator is supplied to either resistive or inductive load. The induction generator excited by the fixed capacitor banks and SVC composed of the TSC and the TCR which is controlled by the feedback PI controller closed

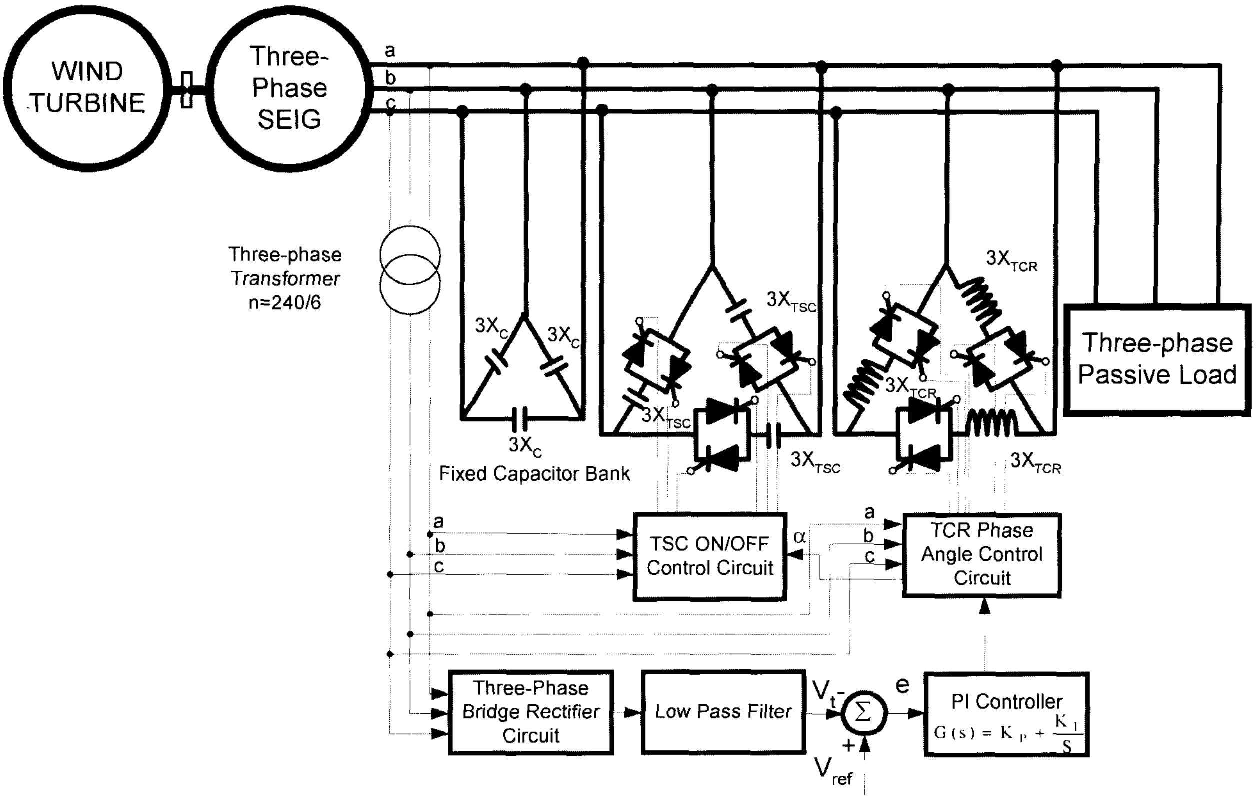

Fig. 2 A Schematic diagram of the three-phase SEIG driven by variable speed prime mover with SVC(TCR-TSC/FC types)controlled by PI controller.

loop circuit designed for regulating the terminal voltage of the three-phase self-excited induction generator. The induction generator is able to be directly driven by a variable speed prime mover as the wind turbine used widely in the renewable and sustainable energy utilizations.

3. SVC with PI Controller For Output Voltage Regulation

Fig.2 shows the static VAR compensator SVC composed of the thyristor phase controlled reactor TCR is implemented for the output voltage regulation of the three-phase SEIG. The instantaneous current flowing through the inductor in the TCR for different triggering angle α is expressed by[13],

$$i_{TCR}(t) = \begin{cases} \dfrac{\sqrt{2}V_t}{X_{TCR}}(\cos\alpha - \cos\omega t) & \alpha \le \omega t \le \alpha + \sigma \\ 0 & \sigma + \alpha \le \omega t \le \alpha + \pi \end{cases} \quad (1)$$

where α is the thyristors delayed angle with respect to zero crossing voltage waveforms, σ is the conduction angle of the thyristors, X_{TCR} is the equivalent inductive reactance of the TCR inductor. V_t is the effective value of the three-phase SEIG terminal voltage. The fundamental component of the inductive reactor current through the TCR which is given by the above equation is obtained on the basis of using the Fourier series expansion,

$$I_{TCR1} = \frac{\sigma - \sin\sigma}{\pi X_{TCR}} V_t \quad (2)$$

where

$$\alpha + \frac{\sigma}{2} = \pi \quad (3)$$

The eqn.(2) can be written as a function of the inductive susceptance of the TCR,

$$I_{RTC1} = B_{TCR}(\sigma)V_t \quad (4)$$

where B_{TCR} is an equivalent inductive susceptance of the TCR and a function of the conduction angle σ(rad) and it is given by,

$$B_{TCR}(\sigma) = \frac{\sigma - \sin\sigma}{\pi X_{TCR}} \quad (5)$$

Observing eqn.(5), the maximum value of B_{TCR} is $1/X_{TCR}$ and occurs when σ is equal to π i.e. α is equal to $\pi/2$.

The Laplace transformation-based transfer function of the PI controller in the voltage regulation loop is represented by,

$$G(s) = K_P + \frac{K_I}{S} \tag{6}$$

where K_P is the proportional gain and K_I is the integral gain.

The input signal to the PI controller is estimated by,

$$E(s) = V_{ref}(s) - V_t(s) \tag{7}$$

where E(s) is the Laplace transformation of the output voltage error, $V_{ref}(s)$ is the Laplace transformation of the reference voltage $V_{ref}(t)$and $V_t(s)$ is the Laplace transformation of the per-phase output voltage $V_t(t)$ of the three-phase SEIG.

The Laplace transformation of the output signal of the PI controller is indicated by,

$$\alpha(s) = E(s)(K_P + \frac{K_I}{S}) \tag{8}$$

The above equation can be expressed in the discrete form by,

$$\alpha(k) = \alpha(k-1) + (K_P + \Delta T K_I)E(k) - K_P E(k-1) \tag{9}$$

where E(k) is the terminal voltage error signal $V_{ref}(k)$-$V_t(k)$at a time sample k, E(k-1) is the error signal at a time sample (k-1), ΔT is the sampling period(sec). When the α is calculated by the PI controller, the conduction angle σ could be obtained and then B_{TCR} can be determined.

4. Torque-Speed Characteristics of Variable Speed Prime Mover

The mechanical output power P_m of the prime mover due to a dc motor which is used as a variable speed prime mover is defined by,

$$P_m = T_a \omega \tag{10}$$

where ω is the angular velocity(rad/sec)and it is expressed by,

$$\omega = \frac{2\pi N_s}{60} \upsilon \tag{11}$$

where v is the per unit speed (v=N/Ns) , N is the rotor shaft speed and N_s is the synchronous speed =1500 rpm and T_a is the mechanical torque (N.m), and it is expressed by,

$$T_a = K_t \phi_m I_a \tag{12}$$

where K_t is the torque constant , ϕ_m is the field flux per pole in wb, and I_a is the armature current of the dc motor which is defined as,

$$I_a = \frac{V_a - K_f \phi_m N}{R_a} \tag{13}$$

where V_a is the armature voltage in Volt , K_f is the field constant and R_a is the armature resistance in ohm , substituting I_a from eqn.(13) to eqn.(12) the following equation which relates the developed dc motor torque with the motor speed N,

$$T_a = K_t \frac{\phi_m}{R_a}(V_a - K_f \phi_m N) \tag{14}$$

The above equation is expressed as a function of the armature rotor shaft speed in per unit,

$$T_m = t_o - \upsilon_o \upsilon \tag{15}$$

where t_o and v_o are torque and speed coefficients defined as,

$$t_o = \frac{K_t \phi_m V_a}{R_a} \tag{16}$$

$$\upsilon_o = \frac{2\pi K_t^2 \phi_m^2}{60 R_a} N_s \tag{17}$$

where $K_f = 2\pi K_t/60$, by substituting from eqn.(11) and eqn.(14) into eqn.(10), the following relation can be obtained by,

$$P_m = (t_o - \upsilon_o \upsilon)(\frac{2\pi N_s}{60})\upsilon \tag{18}$$

The dc motor is separately excited with constant armature voltage and field current control to simulate the characteristics of the wind turbine.

5. Steady State Analysis of Variable Speed Prime Mover Coupled Three-Phase SEIG

The equations representing the steady state performance of the three-phase SEIG driven by the variable speed prime mover can be obtained as follows

From the per-phase approximate equivalent circuit illustrated in Fig.1, the rotor current I_2 referred to the stator side of the three-phase SEIG can be expressed as follows,

$$I_2 = \frac{(f-\upsilon)E_1}{\sqrt{R_2^2 + (f-\upsilon)^2 X_2^2}} \tag{19}$$

where E_1 is the air gap voltage per phase, R_2 and X_2 are resistance and leakage reactance of the rotor referred to the stator side in ohm , respectively. The per unit frequency f=F/50.0 where F is the output frequency of the three-phase SEIG. The term (f-v) is usually very small. Therefore, the term $(f-v)^2X_2^2$ can be substantially neglected with respect to the term R_2^2. Thus, the above equation of the rotor current is able to be reduced to the following equation, That is,

$$I_2 = \frac{(f-\upsilon)E_1}{R_2} \tag{20}$$

The input mechanical power of the three-phase SEIG can be written as[10]

$$P_i = -3I_2^2 \frac{R_2}{(f-\upsilon)}\left(\frac{\upsilon}{f}\right) \tag{21}$$

By substituting I_2 in eqn.(20) into eqn.(21) and making a mechanical power invariance through equating eqn.(18) and eqn.(21) in addition to the resultant expression for the per unit speed v can be obtained by,

$$\upsilon = \frac{m_2 f}{m_1 f + m_3} \tag{22}$$

where m_1, m_2 and m_3 are defined in appendix A.

By using the nodal admittance approach between the nodes C and D, the following equation can be written as follows,

$$(Y_{CD} + Y_{CE} + Y_{CB})E_1 = 0 \tag{23}$$

But E_1 is not equal to zero for the voltage building up successfully, the relationship of the following nodal admittance holds;

$$Y_{CD} + Y_{CE} + Y_{CB} = 0 \tag{24}$$

where Y_{CD}, Y_{CE} and Y_{CB} can be represented by using the equivalent circuit as follows;

$$Y_{CB} = \frac{1}{\dfrac{\left(\dfrac{R_L}{f} + jX_L\right)\left(\dfrac{-jX_C}{f^2}\right)}{\dfrac{R_L}{f} + j\left(X_L - \dfrac{X_C}{f^2}\right)} + \dfrac{R_1}{f} + jX_1} \tag{25}$$

$$Y_{CE} = -\frac{j}{X_m} \tag{26}$$

and

$$Y_{CD} = \frac{1}{\left[\dfrac{R_2}{f-\upsilon} + jX_2\right]} \tag{27}$$

where R_1 and X_1 are the resistance and the leakage reactance of the stator in ohm, respectively, R_L and X_L are the load resistance and reactance in ohm, respectively and X_C=(1/100πC; f=50Hz).On the other hand, the C is the terminal excitation capacitor capacitance denoted in farad and v is defined by eqn.(22)

Equating the sum of the imaginary terms in eqn.(24)to zero, the magnetizing reactance can be obtained as,

$$X_m = \frac{1}{B_{CD} + B_{CB}} \tag{28}$$

and then equating the sum of the real terms of eqn.(24)to zero, the 8^{th} order polynomial function in the per unit frequency f can be written by,

$$\begin{aligned} &Y_8 f^8 + Y_7 f^7 + Y_6 f^6 + Y_5 f^5 + Y_4 f^4 \\ &+ Y_3 f^3 + Y_2 f^2 + Y_1 f + Y_0 = 0 \end{aligned} \tag{29}$$

where B_{CD},B_{CB} and the nine coefficients Y_0 to Y_8 are derived and given in the appendix A.

From eqn.(29) the per-unit frequency f can be determined using Newton Raphson method. From eqn.(28) the magnetizing reactance Xm is also estimated and the air gap voltage E_1 is evaluated from the magnetization characteristic which is the relationship between the air gap voltage E_1 and the magnetizing reactance X_m as evaluated from a synchronous speed test. The three-phase induction machine is driven by the dc motor at synchronous speed corresponding to 50Hz base frequency[3-10]. For the digital computer simulation, the curve is fitted to the linear equations using curve fitting function of the MATLAB software program, the following equation is obtained by,

$$E_1 = \begin{cases} 207.2 - 3.773X_m & X_m \le 24.2 \\ 541.7 - 17.79X_m & 24.2 \le X_m \le 26.5 \\ 0 & X_m \ge 26.5 \end{cases} \quad (30)$$

The following equations are used for estimating the three-phase SEIG performances, that is,

$$V_t = fE_1 \frac{\left| \frac{1}{Y_{CB}} - \left(\frac{R_1}{f} + jX_1\right) \right|}{\left| \frac{1}{Y_{CB}} \right|} \quad (31)$$

$$I_L = \frac{V_t}{\sqrt{R_L^2 + f^2 X_L^2}} \quad (32)$$

$$P_L = 3I_L^2 R_L \quad (33)$$

and

$$Q_L = 3fI_L^2 X_L \quad (34)$$

where V_t, I_L, P_L and Q_L are the per-phase terminal generated voltage, the per-phase load current of the three-phase SEIG , the active and reactive load power, respectively.

6. Voltage Regulation Analysis of Three-Phase SEIG with SVC

The SVC composed of the TSC and the TCR is used for realizing the closed loop voltage regulator of the three-phase SEIG. The conventional fixed-gain PI controller is built for controlling the equivalent susceptance of the TCR and the desired number of capacitors of the TSC. As mentioned above, the equivalent susceptance of the TCR controlled by the PI controller is changed on-line to minimize the terminal voltage error. The three-phase SEIG equivalent circuit with the equivalent susceptance of TCR which is a function of the thyristor triggering conduction angle σ of the TCR is modified as depicted in Fig.3 and the capacitive capacitor reactance of the TSC is conveniently added to the excitation terminal fixed capacitor. The steady-state analysis of the three-phase SEIG system controlled by the SVC connected to its terminal is derived by,

For a given excitation capacitor capacitance, load impedance, machine parameters and torque–speed characteristics of a variable speed prime mover; dc motor, two non-linear simultaneous equations in the per-unit frequency f and the magnetizing reactance X_m are obtained with susceptance controlled by the SVC, B_{TCR} and X_{TSC} paralleled with the load impedance, Y_{CD}, Y_{CE}, Y_{CB} can be expressed using the equivalent circuit as follows,

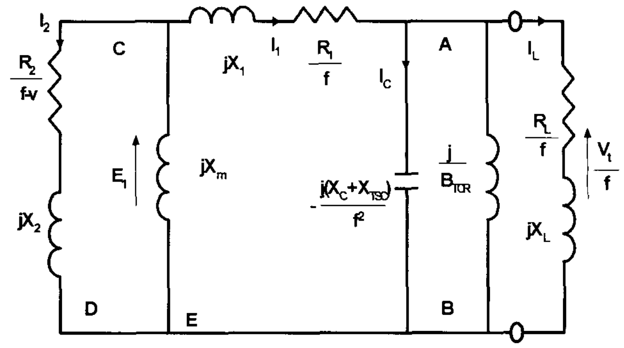

Fig. 3 Per-phase equivalent circuit of three-phase SEIG with additional SVC susceptance

$$Y_{CB} = \frac{1}{\dfrac{\left(\frac{R_L}{f} + jX_L\right)(-jX_{SVC})}{\frac{R_L}{f} + j(X_L - X_{SVC})} + \frac{R_1}{f} + jX_1} \quad (35)$$

where $X_{SVC} = \dfrac{X_C + X_{TSC}}{f^2 - B_{TCR}(X_C + X_{TSC})}$

$$Y_{CE} = -\frac{j}{X_m} \quad (36)$$

and

$$Y_{CD} = \frac{1}{\left[\frac{R_2}{f - \upsilon} + jX_2\right]} \quad (37)$$

By applying the nodal admittance approach and equating the sum of the imaginary terms in eqn.(24) to zero, the magnetizing reactance X_m can be obtained by,

$$X_m = \frac{1}{B_{CD} + B_{CB}} \quad (38)$$

and then equating the sum of the real terms of eqn.(24)to zero, the 10^{th} order polynomial function with respect to the per unit frequency f can be written by,

$$Y_{10}f^{10} + Y_9 f^9 + Y_8 f^8 + Y_7 f^7 + Y_6 f^6 + Y_5 f^5 + Y_4 f^4 + Y_3 f^3 + Y_2 f^2 + Y_1 f + Y_0 = 0 \quad (39)$$

where B_{CD},B_{CB} and the eleven coefficients Y_0 to Y_{10} are derived and provided in the appendix B.

From eqn.(39), the per-unit frequency f can be determined by using Newton Raphson method and then air gap voltage E_1 is evaluated from eqn.(30). The three-phase SEIG Performances the per-phase terminal voltage of the three-phase SEIG , the per-phase load Current, and the active and reactive load power can be respectively calculated by using,

$$V_t = fE_1 \frac{\left| \frac{1}{Y_{CB}} - \left(\frac{R_1}{f} + jX_1\right) \right|}{\left| \frac{1}{Y_{CB}} \right|} \tag{41}$$

$$I_L = \frac{V_t}{\sqrt{R_L^2 + f^2 X_L^2}} \tag{42}$$

$$P_L = 3I_L^2 R_L \tag{43}$$

and

$$Q_L = 3fI_L^2 X_L \tag{44}$$

7. Conclusions

The present paper has introduced an algorithm for steady-state frequency domain analysis and characteristic formulas of the three-phase SEIG stand-alone system which is driven by variable speed prime-mover. The steady-state performances of the three-phase SEIG have obtained in terms of the variations of the terminal output voltage in accordance with output power and prime-mover speed. Furthermore, this paper has presented a static VAR controller requirement for voltage regulation of the three-phase SEIG.

References

[1] Michael Liwschitz-Garik and Clyde C.Whipple, "Alternating current Machines", D.Van Nostrand company, NJ, 1961.

[2] A.F.Puchstein, T.C.Lioyd and A.G.Conard, "Alternating current Machines", John Wiley, 1954.

[3] M.Konstenko and L.Piotravsky, "Electrical Machines", Mir Publishers, Moscow, 1969.

[4] Bhim Singh, "Induction Generator- a Prospective", Electric Machines and Power Systems, Vol.23, pp.163-177, 1995.

[5] M.Ermis, H.B.Erton, M.Demirekler, B.M.Saribatir, Y.Uctvg, M.E.Sezer and I.Cadirici, "Various Induction Generator Schemes for Wind-Electricity Generation", Electric Power Systems Research, Vol.23, pp.71-83, 1992.

[6] A.A.Shaltout and M.A.Adel-Halim, "Solid State Control of Wind-Driven Self-Excited Induction Generator", Electric Machines and Power Systems, Vol.23, pp.571-582, 1995.

[7] T.F.Chan, "Analysis of Self-Excited Induction Generator Using an Iterative Method", IEEE Trans. On Energy Conversion, Vol.EC-10, No.3 pp.502-507, September, 1985.

[8] S.P.Singh, M.P.Jain and Bhim Singh, "A New Technique for Analysis of Self-Excited Induction Generator", Electric Machine and Power Systems, Vol.23, pp647-656, 1995.

[9] T.F.Chan, "Capacitance Requirements of Self-Excited Induction Generators", IEEE Trans. On Energy Conversion, Vol.8, No.2 pp.304-311, June, 1993.

[10] S.Rajakarvna and R.Bonert, "A Technique for The Steady state Analysis of Self-Excited Induction Generator with variable speed", IEEE Trans. On Energy Conversion, Vol.10, No.1, pp.10-16, March, 1995.

[11] W. Koczara, et al: " Variable Speed Three-Phase Power Generation Set", EPE-2001, 2001.

[12] A. Koyanagi et al: "Maximum Power Point Tracking of Wind Turbine Generator Using a Flywheel", Proceedings of the 2001 Japan Industry Application society Conference, Vol.1, pp395-398, 2001.

[13] IEEE Special Stability Controls Working Group Report, "Static VAR Compensator Models for Power Flow and Dynamic Performance Simulation", IEEE Transactions on Power Systems, Vol.9, No.1 February, 1994

Appendix A

$$Y_{CD} = \frac{1}{\frac{R_2}{f - v} + jX_2}$$

$Y_{CD}=G_{CD}+jB_{CD}$

$$G_{CD} = \frac{(A_0 + A_1 f + A_2 f^2)f}{T_0 + T_1 f + T_2 f^2 + T_3 f^3 + T_4 f^4}$$

where

$T_0=G_0^2$, $T_1=2G_0G_1$, $T_2=G_1^2+G_2^2X_2^2$, $T_3=2G_2G_3X_2^2$, $T_4=G_3^2X_2^2$

$A_0=G_0G_2$, $A_1=G_1G_2+G_0G_3$, $A_2=G_1G_3$

And $G_0=R_2m_3$, $G_1=R_2m_1$, $G_2=-t_0$, $G_3=m_1$

$m_1=m_0N_s$, $m_2=180E_1^2/(2\pi N_sR_2)+t_0$, $m_3=180E_1^2/(2\pi N_sR_2)$, $m_0=0.0884$, $t_0=120.08$
where $N_s=1500$ rpm

$$Y_{CB}=\frac{1}{\frac{R_1}{f}+jX_1+(\frac{\frac{-JX_C}{f^2}(\frac{R_L}{f}+jX_L)}{\frac{R_L}{f}+j(X_L-\frac{X_C}{f^2})}}$$

$Y_{CB}=G_{CB}+jB_{CB}$

$$G_{CD}=\frac{D_1f+D_3f^3+D_5f^5}{D_0+D_2f^2+D_4f^4+D_6f^6}$$

where
$D_0=Z_0^2$, $D_2=Z_1^2+2Z_0Z_2$, $D_4=Z_2^2+2Z_3Z_1$, $D_6=Z_3^2$, $D_1=-X_CZ_0$, $D_3=R_LZ_1+X_LZ_0-Z_2X_C$
$D_5=R_LZ_3+X_LZ_2$
$C_0=-Z_1X_C-R_LZ_0$, $C_2=Z_1X_L-Z_3X_C-Z_2R_L$, $C_4=Z_3X_L$
$Y_0=T_0D_1+A_0D_0$, $Y_1=T_1D_1+A_1D_0$,
$Y_2=T_2D_1+T_0D_3+A_0D_2+A_2D_0$, $Y_3=T_3D_1+T_1D_3+A_1D_2$
$Y_4=T_4D_1+T_2D_3+T_0D_5+A_0D_4+A_2D_2$, $Y_5=T_3D_3+T_1D_5+A_1D_4$,
$Y_6=T_4D_3+T_2D_5+A_0D_6+A_2D_4$
$Y_7=T_3D_5+A_1D_6$, $Y_8=T_4D_5+A_2D_6$

$$X_m=\frac{1}{B_{CD}+B_{CB}}$$

where

$$B_{CD}=\frac{(Q_0+Q_1f+D_2f^2)f^2}{T_0+T_1f+T_2f^2+T_3f^3+T_4f^4}$$

$Q_0=-G_2^2X_2$, $Q_1=-2G_2G_3X_2$, $Q_2=-G_3^2X_2$

$$B_{CB}=\frac{(C_0+C_2f^2+C_4f^4)f^2}{D_0+D_2f^2+D_4f^4+D_6f^6}$$

$Z_0=-R_1X_C-X_CR_L$, $Z_1=X_CX_L+X_1X_C+R_1R_L$, $Z_2=R_1X_L+X_1R_L$, $Z_3=-X_1X_L$

Appendix B

$$Y_{CB}=\frac{1}{\frac{R_1}{f}+jX_1+(\frac{\frac{-JX_C+X_{TSC}}{f^2-X_CB_{SVC}}(\frac{R_L}{f}+jX_L)}{\frac{R_L}{f}+j(X_L-\frac{X_C+X_{TSC}}{f^2-X_CB_{SVC}})}}$$

$Y_{CB}=G_{CB}+jB_{CB}$

$$G_{CD}=\frac{(D_0+D_2f^2+D_4f^4+D_6f^6)f}{P_0+P_2f^2+P_4f^4+P_6f^6+P_8f^8}$$

where
$F_0=-R_1X_CR_LB_{TCR}$
$F_2=X_CX_L+X_1X_C+R_1R_L+X_1X_CX_LB_{TCR}$
$F_4=-X_1X_L$
$T_{01}=-R_1X_C-X_CR_L-R_1X_CX_LB_{TCR}-X_1X_CR_LB_{TCR}$
$T_{21}=R_1X_L+X_1R_L$
$P_0=F_0^2$
$P_2=2F_0F_2+T_{01}^2$
$P_4=2F_0F_4+F_2^2+2T_{01}T_{21}$
$P_6=2F_2F_4+T_{21}^2$
$P_8=F_4^2$
$D_0=B_{TCR}F_0$
$D_2=R_LF_0-B_{TCR}X_CR_LF_2-X_CT_{01}(X_LB_{TCR}+1)$
$D_4=R_LF_2-B_{TCR}X_CR_LF_4-X_CT_{21}(X_LB_{TCR}+1)+X_LT_{01}$
$D_6=R_LF_4+X_LT_{21}$
$Y_0=T_0D_0+A_0P_0$
$Y_1=T_1D_0+A_1P_0$
$Y_2=T_0D_2+T_2D_0+A_0P_2+A_2P_0$
$Y_3=T_1D_2+T_3D_0+A_1P_2$
$Y_4=T_0D_4+T_2D_2+T_4D_0+A_0P_4+A_2P_2$
$Y_5=T_1D_4+T_3D_2+A_1P_4$
$Y_6=T_0D_6+T_2D_4+T_4D_2+A_0P_6+A_2P_4$
$Y_7=T_1D_6+T_3D_4+A_1P_6$
$Y_8=T_2D_6+T_4D4+A_0P_8+A_2P_6$
$Y_9=T_3D_6+A_1P_8$
$Y_{10}=T_4D_6+A_2P_8$

$$B_{CB}=\frac{(C_0+C_2f^2+C_4f^4+C_6f^6)f^2}{P_0+P_2f^2+P_4f^4+P_6f^6+P_8f^8}$$

$C_0=T_{01}B_{TCR}X_CR_L-X_CF_0(X_LB_{TCR}+1)$
$C_2=-R_LT_{01}+B_{TCR}X_CR_LT_{21}+X_LF_0-X_CF_2(X_LB_{TCR}+1)$
$C_4=-T_{21}R_L+X_LF_2-X_CF_4(X_LB_{TCR}+1)$
$C_6=F_4X_L$

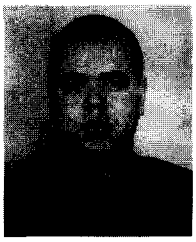

Tarek Ahmed
He received his M Sc.-Eng from the Electrical Engineering Department, Assiut University, Egypt in 1998. He is currently a Ph. D. candidate student in the Graduate School of Science and Engineering, the Power Electronic System and Control Engineering Laboratory at Yamaguchi University, Yamaguchi, Japan. His research interests are in the area of the new applications for the power electronic circuits and systems with the renewable energy and power systems and semiconductor power conditioners. Mr. Ahmed is a student-member of the IEEE and the Japan Society of the Power Electronics.
Tel: +81-836-85-9472 Fax: +81-836-85-9401

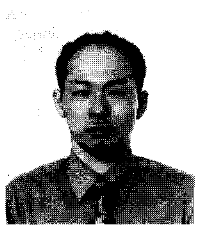

Shinichiro Nagai
He received his B.Sc.-Eng in Mechanical Engineering from Aoyama University in 1995 and joined for a research member in R&D of SANKEN Electric Co., Ltd. He is now a Ph. D. candidate student with the Power Electronic Systems Engineering in the Graduate School of Science and Engineering, Yamaguchi University, Yamaguchi, Japan. He is interested in soft switching inverter and rectifier systems, wind power generation systems and their related digital control systems. Mr. Nagai is a member of the Japan Society of the Power Electronics.

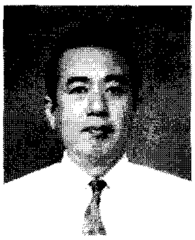

Koji Soshin
He received his M.Sc.-Eng from the Electronic Engineering Department, the Graduate School of Electrical and Electronics Engineering,. Kobe University, Kobe, Japan. He joined Matsushita Electric Works, Ltd. in 1979. He is interested in stepping motor applications, vector controlled inverter for the induction motor and power electronic circuits and systems technologies. He are now working in the power supplies for electric vehicle. He is now a Ph. D. candidate student in the Graduate School of Science and Engineering, Yamaguchi University, Yamaguchi, Japan. Mr. Soshin is a member of the Japan Society of Power Electronics.

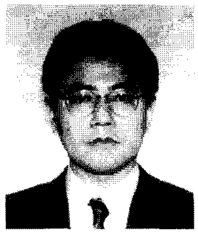

Eiji Hiraki
He received his M. Sc.-Eng in Electrical Engineering from Osaka University, Osaka, Japan in 1990. He is currently with the Power Electronic System and Control Engineering Laboratory at Yamaguchi University, Yamaguchi, Japan, as a Research Associate. His research interests are in the soft-switching technique for high frequency switching power conversion systems. Mr. Hiraki is a member of IEE-Japan, the Japan Society of the Power Electronics and IEEE.

Mutsuo Nakaoka
He received his Dr-Eng. degree in Electrical Engineering from Osaka University, Osaka, Japan in 1981. He joined the Electrical and Electronics Engineering Department of Kobe University, Kobe, Japan in 1981. Since 1995, he has been a professor of the Electrical and Electronics Engineering Department, the Graduate School of Science and Engineering, Yamaguchi University, Yamaguchi, Japan. His research interests include application developments of power electronics circuit and systems. He received the 2001 premium paper award from IEE-UK and so on. Dr. Nakaoka is a member of the Institute of Electronics, Information and Communication Engineers of Japan, Institute of Illumination Engineering of Japan, European Power Electronics Association, the Japan Society of the Solar Energy, IEE-Korea and IEEE.